

Remote Halogen switch of amine hydrophilicity

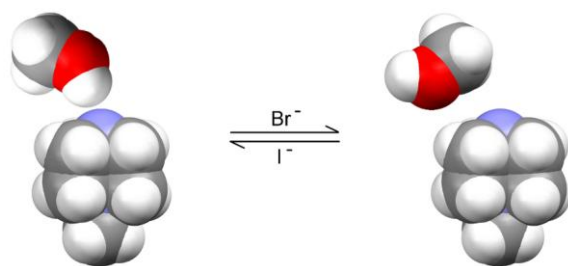
Michał Andrzejewski, Anna Olejniczak, Andrzej Katrusiak*

Faculty of Chemistry, Adam Mickiewicz University, Grunwaldzka 6, 60-780 Poznań, Poland

Corresponding author: katran@amu.edu.pl

Abstract

Bromide and iodide anions switch over the hydrogen-bonding patterns in otherwise isostructural crystals of dimethanol solvate N-methyl-1,4-diazabicyclo[2.2.2]octanium bromide ($\text{dabcoCH}_3\text{Br}\cdot 2\text{CH}_3\text{OH}$) and analogous iodide ($\text{dabcoCH}_3\text{I}\cdot 2\text{CH}_3\text{OH}$), both synthesized in high-pressure Menshutkin reaction at 1.2 GPa and 2.4 GPa, respectively. Magnitudes of pressure triggering these reactions correspond to identical molecular volume of both solvates.



Experimental

Crystals growth at high pressure

High-pressure reactions of $\text{dabcoHBr}/\text{dabcoHI}$ substrate dissolved in an excess of methanol have been conducted *in situ* in a diamond-anvil cell (DAC) [16]. Pressure was calibrated by the ruby-fluorescence method [17] using a Betsa PRL spectrometer, with an accuracy of 0.05 GPa. The gaskets were made of steel foil, 0.11 mm thick, with an aperture of 0.36 mm in diameter. One third of the DAC-chamber volume was filled with few grains of the compound and topped up with methanol. Both samples were prepared in this manner. The yield of both reactions could be assessed of the sizes of the grown single crystals as close to 100%. The pressure triggering reaction was measured in a series of crystallizations at gradually increased pressure, until at 1.2 GPa a new crystal habit was noted (Fig. S1). The subsequent X-ray diffraction measurement confirmed that $\text{dabcoCH}_3\text{Br}\cdot 2\text{CH}_3\text{OH}$ was formed. Another crystal was grown at 1.7 GPa (Fig. S2) and the X-ray diffraction measurement was repeated. The X-ray diffraction powder pattern of the sample recovered from the DAC was inconsistent with $\text{dabcoCH}_3\text{Br}\cdot 2\text{CH}_3\text{OH}$, indicating that the solvate decomposes at 0.1 MPa. Likewise, $\text{dabcoCH}_3\text{I}\cdot 2\text{CH}_3\text{OH}$ was synthesized at 2.4 GPa (Figs S3, S4) and its structure determined at 2.4, 1.2 and 1.0 GPa. Starting from about 1.5 GPa the sample crystal started to dissolve. At 0.8 GPa it broke into small pieces, which could be caused by a phase transition or decomposition, and at 0.5 GPa all the crystalline fragments dissolved completely. Again, X-ray diffraction of the powdered $\text{dabcoCH}_3\text{I}\cdot 2\text{MeOH}$ sample recovered from the DAC was inconsistent with the single crystal structure, indicating the solvate decomposition.

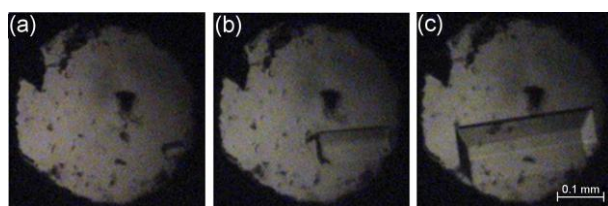


Figure S1. Isochoric growth of a single-crystal of $\text{dabcoCH}_3\text{Br}\cdot 2\text{CH}_3\text{OH}$ from methanol solution: (a) one grain after dissolving polycrystalline precipitate at 383 K; (b) this single crystal at 373 K; (c) 368 K; (d) at 1.2 GPa/296 K.

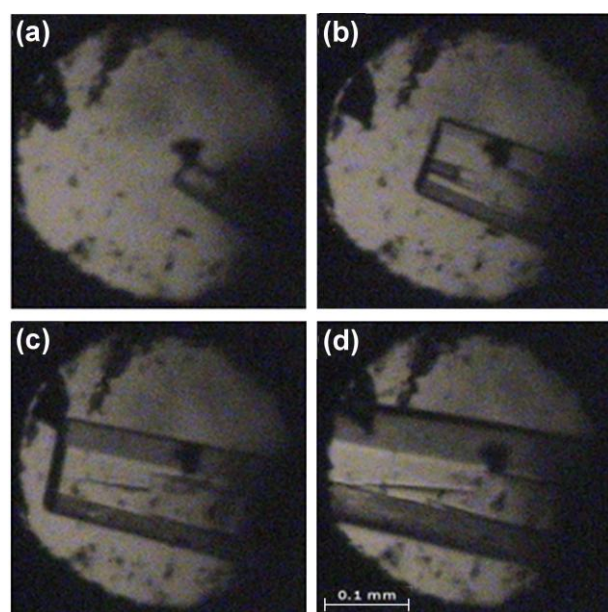


Figure S2. Stages of isochoric growth of a single-crystal $\text{dabcoCH}_3\text{Br}\cdot 2\text{CH}_3\text{OH}$ from methanol solution: (a) one small grain after dissolving polycrystalline mass at 410 K; (b) the same single-crystal at 401 K; (c) 391 K; (d) the single-crystal at 1.7 GPa/296 K.

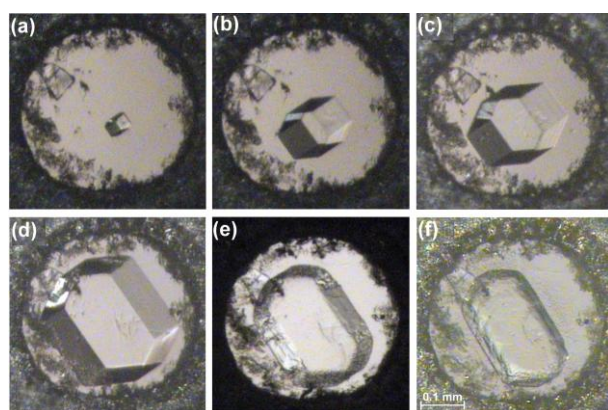


Figure S3. $\text{DabcoCH}_3\text{I}\cdot 2\text{CH}_3\text{OH}$ isochoric crystallization from methanol solution in the DAC chamber: (a) one seed at 453 K, (b) the crystal at 443 K, (c) 423 K, (d) at 2.4 GPa/296 K; and its isothermal dissolution at (e) 1.2 GPa and (f) 1.0 GPa.

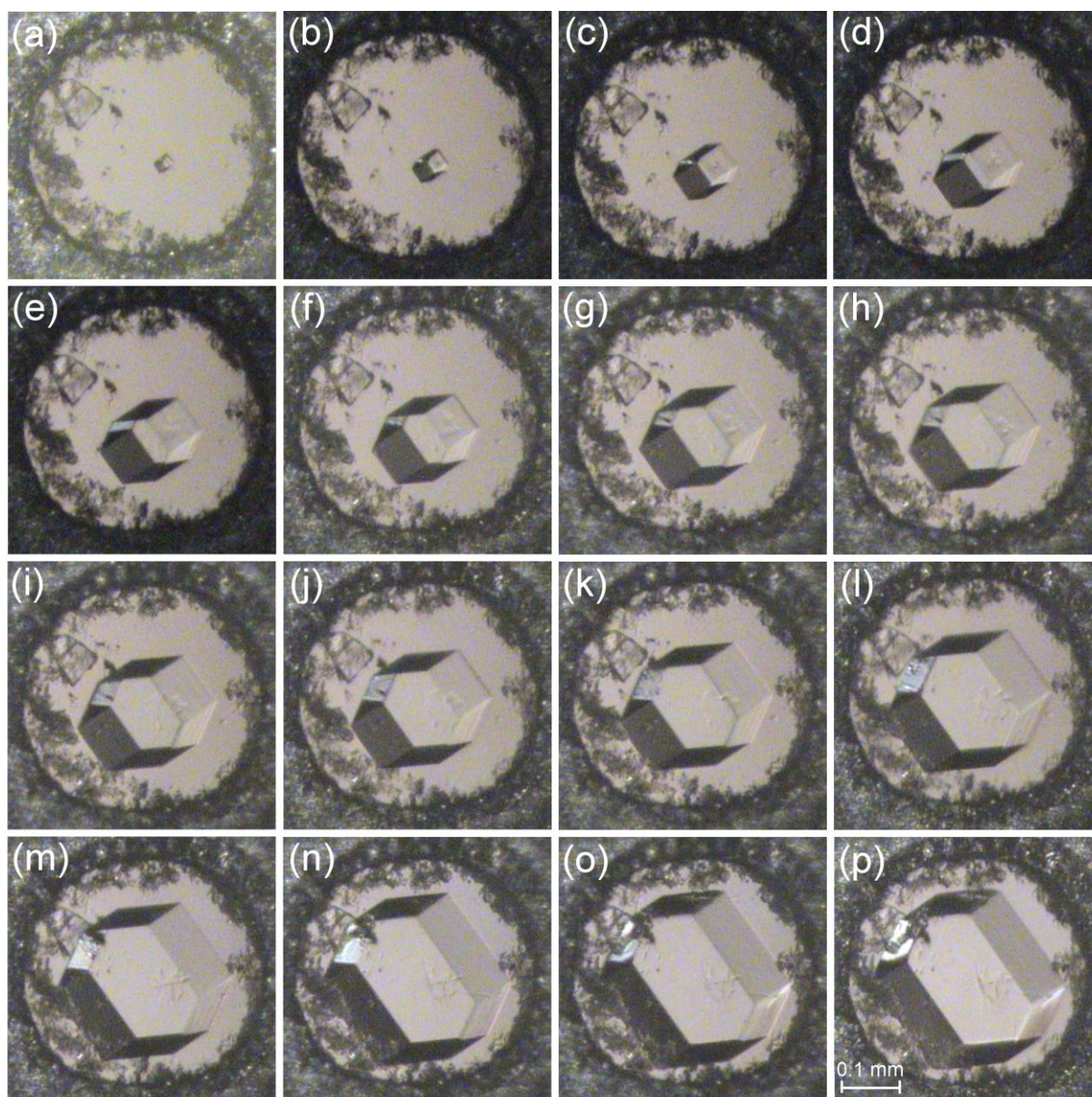


Figure S4. Stages of isochoric growth of the single crystal of dabcoCH₃I·2MeOH from methanol solution: (a) one small grain after dissolving polycrystalline precipitate at 463 K; (b) 453 K; (c-e) 443 K; (f-h) 433 K; (i,j) 423 K; (k) 413 K; (l) 403 K; (m) 373 K; (n) 353 K; (o) 333 K; (p) the single-crystal at 2.4 GPa/296 K.

X-Ray diffraction analyses

The diffraction data of single crystals grown *in situ* in the DAC have been measured with a KUMA KM4-CCD diffractometer according to previously described procedures [18]. The CrysAlis software [19] was used for the data collections and their preliminary reduction. Corrections of intensities for the DAC and sample absorption, and gasket shadowing were applied, and reflections overlapping with diamond reflections were eliminated [20]. All structures were solved straightforwardly by direct methods and refined by full-matrix least-squares [21]. Anisotropic temperature factors were applied for the bromide and iodide anions only. H-Atoms in the structures were located from molecular geometry (AFIX instructions 23,33 and 83), with the C-H distance of 0.97 Å in ethylene, C-H 0.96 Å for methyl, and O-H

0.82 Å for hydroxyl H-atoms, and their U_{iso} 's were constrained to 1.2-1.5 times U_{eq} of the carrier atoms.

Table S1. Crystal data and structure-refinements details of dabcoCH₃Br·2CH₃OH and dabcoCH₃I·2CH₃OH solvates.

	dabcoCH ₃ Br·2CH ₃ OH		dabcoCH ₃ I·2CH ₃ OH		
p (GPa)	1.20(5)	1.70(5)	1.00(5)	1.20(5)	2.40(5)
Formula	C ₉ H ₂₃ N ₂ BrO ₂	C ₉ H ₂₃ N ₂ BrO ₂	C ₉ H ₂₃ N ₂ IO ₂	C ₉ H ₂₃ N ₂ IO ₂	C ₉ H ₂₃ N ₂ IO ₂
T (K)	296(2)	296(2)	296(2)	296(2)	296(2)
Formula weight	271.2	271.2	318.19	318.19	318.19
Wavelength (Å)	0.71073	0.71073	0.71073	0.71073	0.71073
Crystal system	monoclinic	monoclinic	monoclinic	monoclinic	monoclinic
Space group	P2 ₁ /m	P2 ₁ /m	P2 ₁ /m	P2 ₁ /m	P2 ₁ /m
Unit cell dimensions (Å, °)					
a	9.270(2)	9.194(4)	9.059(3)	9.040(3)	8.879(3)
b	6.7304(13)	6.653(3)	6.7868(17)	6.7590(9)	6.6161(9)
c	9.710(4)	9.643(9)	10.543(4)	10.516(3)	10.328(3)
β	107.60(4)	107.72(7)	108.28(3)	108.45(3)	108.81(3)
Volume (Å ³)	577.5(3)	561.9(6)	615.5(3)	609.5(3)	574.3(2)
Z	2	2	2	2	2
Calculated density (g/cm ³)	1.560	1.603	1.717	1.734	1.840
Absorption coefficient (mm ⁻¹)	3.540	3.639	2.584	2.609	2.769
F(000)	284	284	320	320	320
Crystal size (mm)	0.44x0.14x0.10	0.46x0.18x0.10	0.16x0.28x0.10	0.21x0.28x0.10	0.26x0.29x0.10
θ-range for data collection (°)	3.81 to 28.23	3.85 to 28.49	3.57 to 26.85	3.59 to 26.98	3.67 to 28.17
Min/max indices:h, k, l	-11/12,-8/8,-5/5	-12/11,-8/8,-4/4	-5/5,-8/8,-9/9	-5/5,-8/8,-9/9	-5/5,-8/8,-9/9
Reflect. Collected/unique	4082/447	3313/370	2279/221	2345/226	2509/241
Rint	0.1142	0.2220	0.0394	0.0544	0.0789
Refinement method	Full-matrix least-squares on F ²				
Completeness (%)	29.0	24.0	15.3	15.6	15.7
Data/restraints/parameters	447/4/40	370/2/43	221/2/42	226/2/42	241/2/42
Goodness-of-fit on F ²	1.167	1.137	1.178	1.676	1.394
Final R1/wR2 (I>2σ1)	0.0643/0.1434	0.1125/0.2178	0.0258/0.0609	0.0447/0.1544	0.0550/0.0882
R1/wR2 (all data)	0.0984/0.1599	0.1801/0.2507	0.0277/0.0617	0.0486/0.1566	0.0590/0.0884
Weighting parameters w ₁ ,w ₂ ^{a)}	0.0779/0.4758	0.1232/0.0000	0.0336/0.7968	0.0477/0.1549	0.0000/5.5037
Largest diff. peak/hole (e.Å ⁻³)	0.442/-0.377	0.415/-0.346	0.195/-0.196	0.537/-0.540	0.259/-0.236

$$w=1/(\sigma^2 F_o^2+w_1^2 * P^2+w_2 * P), \text{ where } P=(\text{Max}(F_o^2,0)+2 * F_c^2)/3$$

Table S2. The intermolecular and interionic contacts shorter than the sums of van der Waals radii [13] in the structures of dabcoCH₃Br·2CH₃OH and dabcoCH₃I·2CH₃OH solvates. Distances longer than these sums between Br⁻ and C(7)H₃ have been added for comparison (indicated with asterisks).

DH...A	H...A (Å)	D...A (Å)	DH...A (°)	Symmetry code
dabcoCH₃Br·2CH₃OH at 1.2 GPa				
O(1M)-H(1M)···Br(1)	2.59(1)	3.23(8)	124	1-x,2-y,1-z
O(1M)-H(1M)···Br(1)	2.59(1)	3.23(8)	124	1-x,-0.5+y,1-z
*C(7)-H(7A)···Br(1)	3.21(1)	3.80(6)	121	x,y,z
*C(2M)-H(2MC)···Br(1)	3.21(1)	3.60(7)	107	x,y,x
O(2M)-H(2MA)···O(1M)	2.41	4.10(1)	140	1-x,0.5+y,1-z
O(2M)-H(2MC)···O(1M)	2.50	4.10(1)	134	1-x,2-y,1-z
O(2M)-H(2MA)···O(1M)	2.41	4.10(1)	140	1-x,1-y,1-z
O(2M)-H(2MC)···O(1M)	2.50	4.10(1)	134	1-x,-0.5+y,1-z
O(2M)-H(2M)···O(1M)	2.00	2.77(5)	156	x,y,z
O(2M)-H(2M)···O(1M)	2.00	2.77(5)	156	x,y,z
C(5)-H(5B)···O(1M)	2.63	3.46(2)	144	x,y,z
C(5)-H(5B)···O(1M)	2.63	3.46(2)	144	x,1.5-y,1+z
C(7)-H(7B)···O(1M)	2.50	3.45(2)	168	x,1.5-y,1+z
C(7)-H(7B)···O(1M)	2.63	3.45(2)	144	x,y,1+z
C(7)-H(7B)···O(1M)	2.63	3.45(2)	144	x,1.5-y,1+z
C(7)-H(7B)···O(1M)	2.50	3.45(2)	165	x,y,1+z
C(6)-H(6B)···O(2M)	2.63	3.10(2)	110	1-x,2-y,1-z
C(6)-H(6B)···O(2M)	2.63	3.10(2)	110	1-x,-0.5+y,1-z
dabcoCH₃Br·2CH₃OH at 1.7 GPa				
O(1M)-H(1M)···Br(1)	2.55	3.16	122	1-x,2-y,1-z
O(1M)-H(1M)···Br(1)	2.55	3.16	122	1-x,-0.5+y,1-z
*C(7)-H(7A)···Br(1)	3.16(1)	3.51(5)	120	x,y,z
*C(2M)-H(2MC)···Br(1)	3.14(1)	3.74(7)	104	x,y,x
O(2M)-H(2MA)···O(1M)	2.44	4.17	143	1-x,0.5+y,1-z
O(2M)-H(2MC)···O(1M)	2.57	4.17	134	1-x,2-y,1-z
O(2M)-H(2MA)···O(1M)	2.44	4.17	143	1-x,1-y,1-z
O(2M)-H(2MC)···O(1M)	2.57	4.17	134	1-x,-0.5+y,1-z
O(2M)-H(2M)···O(1M)	1.96	2.74	158	x,y,z
O(2M)-H(2M)···O(1M)	1.96	2.74	158	x,y,z
C(5)-H(5B)···O(2M)	2.67	3.19(3)	114	1-x,2-y,1-z
C(5)-H(5B)···O(2M)	2.67	3.19(3)	114	1-x,-0.5-y,1-z
C(7)-H(7B)···O(1M)	2.40	3.35(1)	168	x,1.5-y,1+z
C(7)-H(7B)···O(1M)	2.53	3.35(1)	143	x,y,1+z
C(7)-H(7B)···O(1M)	2.53	3.35(1)	143	x,1.5-y,1+z
C(7)-H(7B)···O(1M)	2.40	3.35(1)	168	x,y,1+z
C(6)-H(6B)···O(2M)	2.63	3.11(5)	111	1-x,2-y,1-z
C(6)-H(6B)···O(2M)	2.63	3.11(5)	111	1-x,-0.5+y,1-z

Table S2. Continuation.

DH...A	H...A (Å)	D...A (Å)	DH...A (°)	Symmetry code
dabcoCH₃I·CH₃OH at 1.0 GPa				
C(7)-H(7A)···I(1)	3.16	4.09(5)	164	x,y,1+z
C(7)-H(7B)···I(1)	3.13	4.06(3)	164	-x,1-y,-z
C(7)-H(7B)···I(1)	3.13	4.06(3)	164	-x,-0.5+y,-z
O(2M)-H(2M)···I(1)	2.77	3.55(3)	159	x,y,z
O(1M)-H(1M)···N(4)	1.97	2.80(4)	178	x,y,z
C(3)-H(3A)···O(1M)	2.67	3.41(1)	135	1-x,1-y,-z
C(5)-H(5A)···O(1M)	2.52	3.28(4)	136	1-x,0.5+y,-z
C(5)-H(5A)···O(1M)	2.52	3.28(4)	136	1-x,-y,-z
C(3)-H(3A)···O(1M)	2.67	3.42(1)	134	1-x,-0.5+y,-z
C(6)-H(6A)···O(2M)	2.62	2.96(3)	100	1-x,0.5+y,-z
C(5)-H(5B)···O(2M)	2.67	2.97(3)	98	1-x,0.5+y,-z
C(5)-H(5B)···O(2M)	2.67	2.97(3)	98	1-x,-y,-z
C(6)-H(6A)···O(2M)	2.62	2.96(3)	100	1-x,-y,-z
dabcoCH₃I·2CH₃OH at 1.2 GPa				
C(7)-H(7A)···I(1)	3.15	4.07(7)	161	x,y,1+z
C(7)-H(7B)···I(1)	3.11	4.03(6)	163	-x,1-y,-z
C(7)-H(7B)···I(1)	3.11	4.03(6)	163	-x,-0.5+y,-z
C(2M)-H(2MB)···I(1)	3.14	4.10(2)	178	1-x,1-y,1-z
C(2M)-H(2MB)···I(1)	3.14	4.10(2)	178	1-x,-0.5+y,1-z
O(2M)-H(2M)···I(1)	2.84	3.62(4)	157	x,y,z
O(1M)-H(1M)···N(4)	2.02	2.84(7)	168	x,y,z
C(3)-H(3A)···O(1M)	2.65	3.39(1)	133	1-x,1-y,-z
C(5)-H(5A)···O(1M)	2.58	3.32(7)	133	1-x,0.5+y,-z
C(5)-H(5A)···O(1M)	2.58	3.32(7)	133	1-x,-y,-z
C(3)-H(3A)···O(1M)	2.65	3.39(1)	133	1-x,-0.5+y,-z
C(6)-H(6A)···O(2M)	2.55	2.90(6)	101	1-x,0.5+y,-z
C(5)-H(5B)···O(2M)	2.67	2.94(5)	96	1-x,0.5+y,-z
C(5)-H(5B)···O(2M)	2.67	2.94(5)	96	1-x,-y,-z
C(6)-H(6A)···O(2M)	2.55	2.90(6)	101	1-x,-y,-z
dabcoCH₃I·2CH₃OH at 2.4 GPa				
C(7)-H(7A)···I(1)	3.09	4.00(7)	160	x,y,1+z
C(7)-H(7B)···I(1)	3.06	3.99(4)	163	-x,1-y,-z
C(7)-H(7B)···I(1)	3.06	3.99(4)	163	-x,-0.5+y,-z
C(2M)-H(2MB)···I(1)	3.07	4.65(2)	177	1-x,1-y,1-z
C(2M)-H(2MB)···I(1)	3.07	4.65(2)	177	1-x,-0.5+y,1-z
C(2M)-H(2MA)···I(1)	3.16	3.82(3)	128	x,y,z
O(2M)-H(2M)···I(1)	2.80	3.56(4)	155	x,y,z
O(1M)-H(1M)···N(4)	1.93	2.75(5)	173	x,y,z
C(3)-H(3A)···O(1M)	2.60	3.33(1)	132	1-x,1-y,-z
C(5)-H(5A)···O(1M)	2.55	3.27(6)	131	1-x,0.5+y,-z
C(5)-H(5A)···O(1M)	2.55	3.27(6)	131	1-x,-y,-z
C(3)-H(3A)···O(1M)	2.60	3.33(1)	132	1-x,-0.5+y,-z
C(6)-H(6A)···O(2M)	2.81	2.84(5)	82	1-x,0.5+y,-z
C(5)-H(5B)···O(2M)	2.61	2.89(4)	97	1-x,0.5+y,-z
C(5)-H(5B)···O(2M)	2.61	2.89(4)	97	1-x,-y,-z
C(6)-H(6A)···O(2M)	2.81	2.84(5)	82	1-x,-y,-z